



Silencing COX-2 blocks PDK1/TRAF4-induced AKT activation to inhibit fibrogenesis during skeletal muscle atrophy

Hongtao Chen^{a,1}, Zhanyang Qian^{b,1}, Sheng Zhang^{a,1}, Jian Tang^{e,1}, Le Fang^c, Fan Jiang^a, Dawei Ge^d, Jie Chang^a, Jiang Cao^a, Lei Yang^{d,**}, Xiaojian Cao^{a,*}

^a Department of Orthopedics, First Affiliated Hospital of Nanjing Medical University, Nanjing, Jiangsu, China

^b Department of Orthopedics, Zhongda Hospital of Southeast University, Nanjing, Jiangsu, China

^c Department of Critical Care Medicine, First Affiliated Hospital of Nanjing Medical University, Nanjing, Jiangsu, China

^d Department of Orthopedics, Nanjing First Hospital, Nanjing Medical University, Nanjing, Jiangsu, China

^e Department of Plastic and Burn Surgery, First Affiliated Hospital of Nanjing Medical University, Nanjing, Jiangsu, China

ARTICLE INFO

Keywords:

COX-2
Skeletal muscle atrophy
Fibrogenesis
PDK1/AKT
TRAF4

ABSTRACT

Skeletal muscle atrophy with high prevalence can induce weakness and fatigability and place huge burden on both health and quality of life. During skeletal muscle degeneration, excessive fibroblasts and extracellular matrix (ECM) accumulated to replace and impair the resident muscle fiber and led to loss of muscle mass. Cyclooxygenase-2 (COX-2), the rate-limiting enzyme in synthesis of prostaglandin, has been identified as a positive regulator in pathophysiological process like inflammation and oxidative stress. In our study, we found injured muscles of human subjects and mouse model overexpressed COX-2 compared to the non-damaged region and COX-2 was also upregulated in fibroblasts following TGF- β stimulation. Then we detected the effect of selective COX-2 inhibitor celecoxib on fibrogenesis. Celecoxib mediated anti-fibrotic effect by inhibiting fibroblast differentiation, proliferation and migration as well as inactivating TGF- β -dependent signaling pathway, non-canonical TGF- β pathways and suppressing generation of reactive oxygen species (ROS) and oxidative stress. In vivo pharmacological inhibition of COX-2 by celecoxib decreased tissue fibrosis and increased skeletal muscle fiber preservation reflected by less ECM formation and myofibroblast accumulation with decreased p-ERK1/2, p-Smad2/3, TGF- β R1, VEGF, NOX2 and NOX4 expression. Expression profiling further found that celecoxib could suppress PDK1 expression. The interaction between COX-2 and PDK1/AKT signaling remained unclear, here we found that COX-2 could bind to PDK1/AKT to form compound. Knockdown of COX-2 in fibroblasts by pharmacological inactivation or by siRNA restrained PDK1 expression and AKT phosphorylation induced by TGF- β treatment. Besides, si-COX-2 prevented TGF- β -induced K63-ubiquitination of AKT by blocking the interaction between AKT and E3 ubiquitin ligase TRAF4. In summary, we found blocking COX-2 inhibited fibrogenesis after muscle atrophy induced by injury and suppressed AKT signaling pathway by inhibiting upstream PDK1 expression and preventing the recruitment of TRAF4 to AKT, indicating that COX-2/PDK1/AKT signaling pathway promised to be target for treating muscle atrophy in the future.

1. Introduction

Skeletal muscle atrophy caused by acute surgical injury always leads to proinflammation and profibrotic factors release, numerous fibroblasts accumulation, extensive collagen cross-linkage and extra cellular matrix (ECM) deposition [1–3]. The process is defined as fibrosis, which results

in significant tissue remodeling that can affect its function [4–6]. Aberrant fibrosis during skeletal muscle atrophy induced by surgical injury even replaces functional and contractile muscle fibers and impairs skeletal muscle regeneration and function [7–10], thus requiring measures to control the abnormal physiological condition [11]. In fact, severe fibrosis of the tissue parenchyma accounts for almost 45% of the

* Corresponding author. Department of Orthopedics, First Affiliated Hospital of Nanjing Medical University, 300 Guangzhou Road, Nanjing, 210029, Jiangsu, China.

** Corresponding author. Department of Orthopedics, Nanjing First Hospital, Nanjing Medical University, No. 68, Changle Road, Nanjing, 210001, Jiangsu, China.
E-mail addresses: leiyang@njmu.edu.cn (L. Yang), xiaojiancao001@163.com (X. Cao).

¹ Authorship note: HC, ZQ, SZ and JT contributed equally to this work.

<https://doi.org/10.1016/j.redox.2020.101774>

Received 17 August 2020; Received in revised form 26 October 2020; Accepted 27 October 2020

Available online 1 November 2020

2213-2317/© 2020 The Author(s).

Published by Elsevier B.V. This is an open access article under the CC BY-NC-ND license

(<http://creativecommons.org/licenses/by-nc-nd/4.0/>).

deaths in developed countries, and significantly reduces the quality of life [12]. Several drugs and biomaterials can attenuate fibrosis after surgery and promote tissue regeneration over scar formation [13–17], but have not been translated to clinical applications.

Fibrosis can be divided into three stages: (a) inflammation, (b) ECM expansion, and (c) tissue remodeling [18,19]. The inflammatory response is triggered by recruitment of effector cells that secrete cytokines and chemokines, including TGF- β that has been defined as a core role of fibrosis by promoting differentiation of fibroblasts to myofibroblasts. The binding of TGF- β to the TGF- β receptor type I activates the downstream canonical signaling Smad2/3 and phosphorylation of Smad2/3 binds to Smad4 and translocated into nucleus to drive activated myofibroblast phenotype and fibrosis-associated gene expression [20,21]. Non-canonical TGF- β (Smad independent) pathways like ERK1/2 (extracellular regulated protein kinase 1/2) of MAPK (mitogen-activated protein kinase) [22], YAP/TAZ (yes-associated protein and transcriptional coactivator with PDZ-binding motif) of Hippo [23] and VEGF (vascular endothelial growth factor) [24] pathways, all of which have been clarified to contribute to fibrotic progression. However, pro-fibrotic effect of TGF- β is not completely blocked after inhibiting these signaling pathways, suggesting that additional factors are essential for signal transduction of TGF- β . Recognition of downstream significant regulators of TGF- β may provide the theory for therapy for fibrotic diseases. Besides, oxidative stress is also required to promote fibrogenesis [25], thus inhibition of generation of ROS could relieve the process of fibrosis.

COX-2 (also known as PTGS2), upon synthesis, localizes to the lumen of the endoplasmic reticulum and nuclear envelope and promotes the synthesis of prostaglandins that induce pain by sensitizing the peripheral and central nociceptors [26]. COX-2 is encoded by genes located on chromosome 1 [27] and contains two separate active sites: 1) cyclooxygenase active site, which increases the oxygenation of polyunsaturated fatty acids to transform to hydroperoxy endoperoxides; 2) peroxidase active site, which decreases the hydroperoxide to synthesize alcohol. COX-2 is normally absent in all tissues and organs but is highly inducible in response to harmful stimuli or cytokine induction, such as inflammation, oxidative stress, autoimmune reactions, mechanical injury and TGF- β stimulation [28]. It regulates cell growth, migration, proliferation, autophagy, apoptosis, immune responses [29–32].

Non-steroidal anti-inflammatory drugs (NSAIDs) prevent the synthesis of PGs from AA by suppressing the cyclooxygenase reactions of COX-1 and COX-2 [33]. Anti-inflammatory and analgesic effects of NSAIDs is principally realized by inhibiting the expression of COX-2 in inflammatory cells [34,35]. Celecoxib, as selective non-steroidal COX-2 inhibitor, was demonstrated to be applied in clinical trial for treatment of diverse tumors including carcinoma of the bladder [36], breast cancer [37], colorectal adenomas [38] and familial adenomatous polyposis [39] and intervention of bipolar depression [40] and arthritis [41]. Inhibition of celecoxib was also verified to ameliorate liver fibrosis [42], tendon tissue fibrosis [43,44] and intra-abdominal adhesion [45], but not investigated in fibrogenesis after skeletal muscle injury induced by surgery. In addition, celecoxib was reported to show anti-fibrotic in various organ fibrosis via inactivating PDK1 (3-phosphoinositide dependent protein kinase-1)/AKT signaling pathway [46]. However, the specific mechanism underlying the interaction between COX-2 and PDK1/AKT remains unclear. The serine/threonine kinase AKT, known as protein kinase B, is phosphorylated and activated by PDK1. The PDK1–Akt signaling induces downstream expression of PI3K and plays a key role in various cellular functions, including cell survival, cell cycle progression, cell polarization, cell migration and microtubule stabilization [47]. AKT regulates a wide range of biological processes and is activated by E3 ubiquitin ligase TRAF4 [48]. K63-linked ubiquitination has been confirmed to be important for AKT activation and transduction by promoting its membrane recruitment. As regulator of Lys63 polyubiquitination, TRAF4 could activate downstream signaling and mediate DNA repair [49]. Here we found COX-2 knockdown inactivated

AKT by inhibiting its upstream signaling PDK1 and blocked recruitment of TRAF4 to activate AKT Lys63 polyubiquitination.

In this study, we demonstrate that COX-2 is hyperactive in injured skeletal muscles and fibroblasts cultured with TGF- β . Pharmacological or genetic inhibition of COX-2 suppresses canonical and non-canonical TGF- β signaling pathways and attenuates tissue fibrosis in skeletal muscle injury models. The results presented here indicate that COX-2 could be target for therapeutic applications of skeletal muscle atrophy.

2. Results

2.1. High levels of COX-2 expression were found in injured muscles

In order to determine whether the expression of COX-2 was induced by muscle injury, we determined COX-2 levels in muscles that had been injured as a result of bone fractures, compared with normal muscles without NSAIDs treatment. Notably, the damaged areas of the muscles showed a greater degree of heterogeneity than the non-injured sites, with respect to levels of COX-2 expression (Fig. 1A). Immunoblotting analysis of muscle tissues confirmed that the injured muscles contained higher COX-2 protein levels than normal muscles (Fig. 1B and C). Parallel studies were performed through surgical incision of muscles in mice. Consistently, muscle tissue from the site of surgery was found to have expressed significantly higher levels of COX-2 protein expression (Fig. 1D and E). Previous studies show that active ECM deposition is principally composed of myofibroblasts to form idiopathic pulmonary fibrosis (IPF) focus [50,51], which polarizes into two parts: active fibrotic front and myofibroblast core. The former is a high-density fibroblast region constitutive of proliferating cells. The latter is composed of noncycling myofibroblasts actively secreting collagen and fibronectin. We conducted immunofluorescent staining for COX-2, α -SMA and collagen I. The analysis verified α -SMA + myofibroblasts and collagen I + ECM in the focus core with low cellular region and COX-2-expressing cells in the active fibrotic front with high cellular region (Fig. S1A–H). We also examined fibroblastic foci for the mesenchymal progenitor cell (MPC) marker S100A4 and proliferating cell marker Ki67, which displays the proliferative mesenchymal progenitor cells of active fibrotic front. Double staining for S100A4 and Ki67 suggested MPC and proliferating cells in the active fibrotic front (Fig. S1I–K), indicating that COX-2-expressing cells in the high cellular density region had the characteristic of MPC.

2.2. Celecoxib exerted inhibitory effect on myofibroblast differentiation and fibrogenesis by inhibiting canonical and non-canonical TGF- β signaling pathways

To further ascertain whether celecoxib participates in the induction of fibroblast differentiation into activated myofibroblasts and secretion of the extracellular matrix (ECM), we investigated the expression of fibrogenesis-associated genes. Myofibroblasts, which are characterized by the expression of α -SMA, produce ECM containing collagen I, III and extra domain A fibronectin (EDA fibronectin) [52–54]. Activation of fibroblasts proceeds in a TGF- β dependent manner. Indeed, recombinant TGF- β significantly increased COX-2 expression both in the nucleus and cytoplasm of fibroblasts, with the maximum level detected after treatment with TGF- β for 24h (Fig. 2A). As expected, western blotting analysis confirmed that TGF- β expression significantly increased the expression of fibrogenesis-regulated genes α -SMA, YAP/TAZ, collagen I, collagen III and fibronectin, as well as COX-2 expression at the protein level (Fig. 2B), suggesting that TGF- β endowed fibroblasts with pro-fibrotic ability. In order to investigate the potential molecular mechanisms underlying analgesic-regulated fibrosis, we focused on the canonical TGF- β signaling like Smad2/3 and non-canonical TGF- β signaling including ERK1/2 and YAP/TAZ pathways, as these kinases has been shown to be closely associated with fibrogenesis [55–57]. Celecoxib elicited a substantial inhibitory effect on COX-2 expression, and

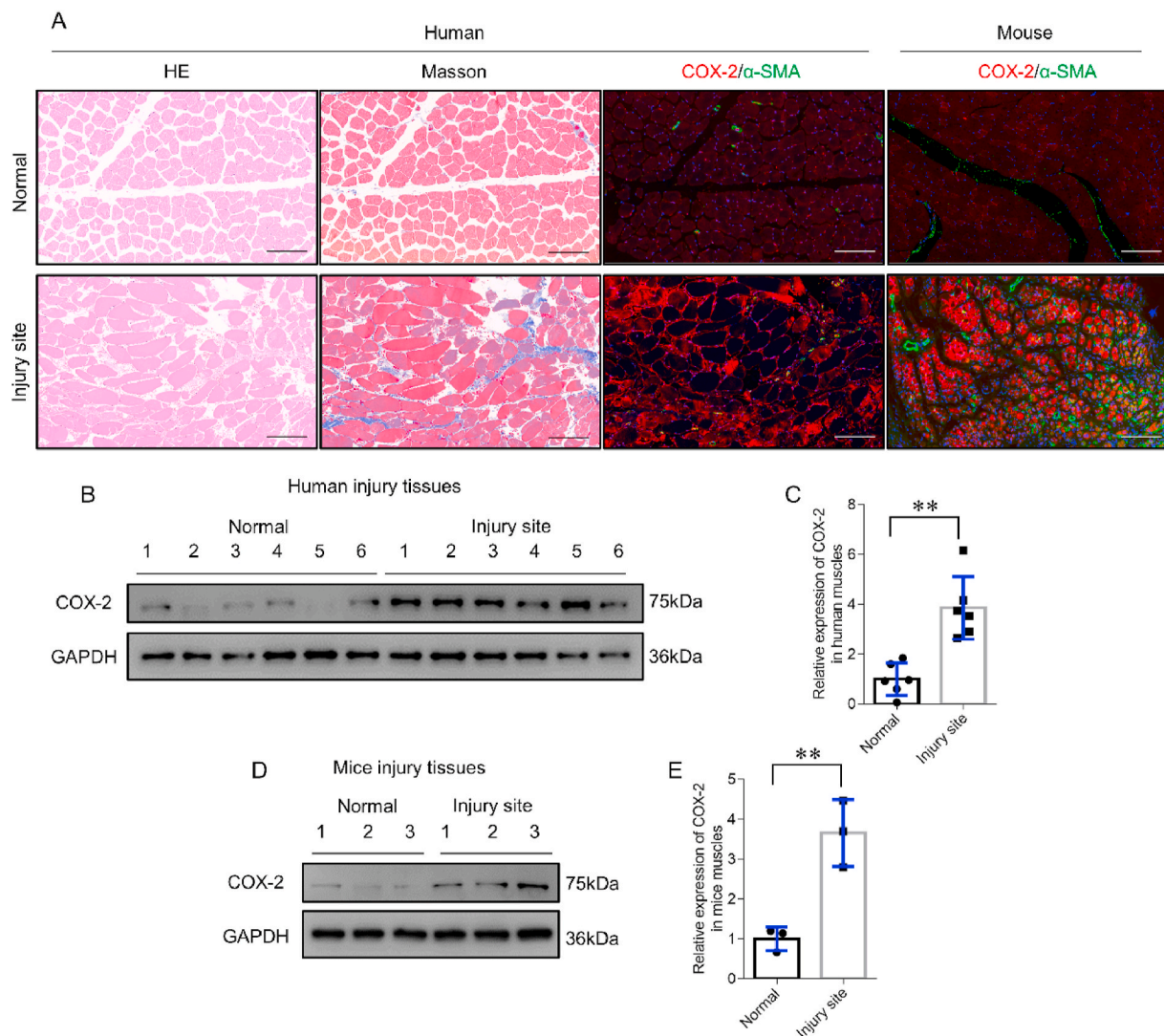


Fig. 1. COX-2 is overexpressed in injured muscle tissues. (A) Representative images of H&E, Masson-stained and fluorescence intensities of COX-2 (Red), α -SMA (Green) and DAPI (Blue) from normal and injured muscle tissues of fracture patients or mouse. Scale bar = 200 μ m. (B) Immunoblot and corresponding bar graphs showing COX-2 levels in the injured and normal muscle tissues from 6 patients. (C) Quantitative analysis of (B). (D) Immunoblot and corresponding bar graphs showing COX-2 levels in injured and normal muscle tissues from 3 mice. (E) Quantitative analysis of (D). Each lane in the blots represents an individual patient- or mouse. Values indicate mean \pm SD. $**p < 0.01$.

subsequently inhibited TGF- β -mediated fibrosis in protein levels (Fig. 2B–D). We employed a dose of 10 nM, based on higher levels of inhibition in the following experiments. Consistent with the suppressive function of celecoxib on COX-2 protein expression, a concentration of 10 nM resulted in a significant decrease in levels of COX-2 and profibrotic gene mRNA expressions (Fig. 2E–J). Immunofluorescence staining further validated the anti-fibrosis effect of celecoxib during fibroblastic differentiation (Fig. 2K).

2.3. Celecoxib inhibited intracellular oxidative stress and fibroblast proliferation and migration

Oxidative stress is essential for the fibrosis pathogenesis at its early stage and high levels of ROS were observed in activated fibroblasts. In the present study, we found that TGF- β induced oxidative stress in fibroblasts by increasing the expression of NOX2 and NOX4 as well as ROS level, while celecoxib showed significantly antioxidant effect against TGF- β (Fig. 3A–D).

The well-known mechanisms of fibrogenesis involve fibroblast proliferation at the permanent location and migration from the wound

injury site [58,59]. Therefore, we observed the effect of celecoxib on fibroblast proliferation and migration. The results of the Edu analysis showed increase levels of proliferation after TGF- β treatment (Fig. 3E). Administration of celecoxib significantly decreased Edu positive cell number and inhibited proliferative effect of TGF- β on fibroblasts (Fig. 3E and F). Furthermore, we further explored fibroblast migration using wound healing experiments and counted the number of cells that had migrated into cell-free gaps. Silencing of COX-2 significantly inhibited directional fibroblast movement into the wound, compared with control cells. Additionally, celecoxib markedly inhibited TGF- β -induced fibroblast movement into the gaps (Fig. 3G and H). In order to determine the regulation effect of celecoxib on directed migration, Transwell chamber assays were employed to detect levels of chemotaxis migration of fibroblasts. We found that fibroblasts treated with TGF- β showed higher number of migrated fibroblasts than control group, and migration was blocked by celecoxib (Fig. 3I and J).

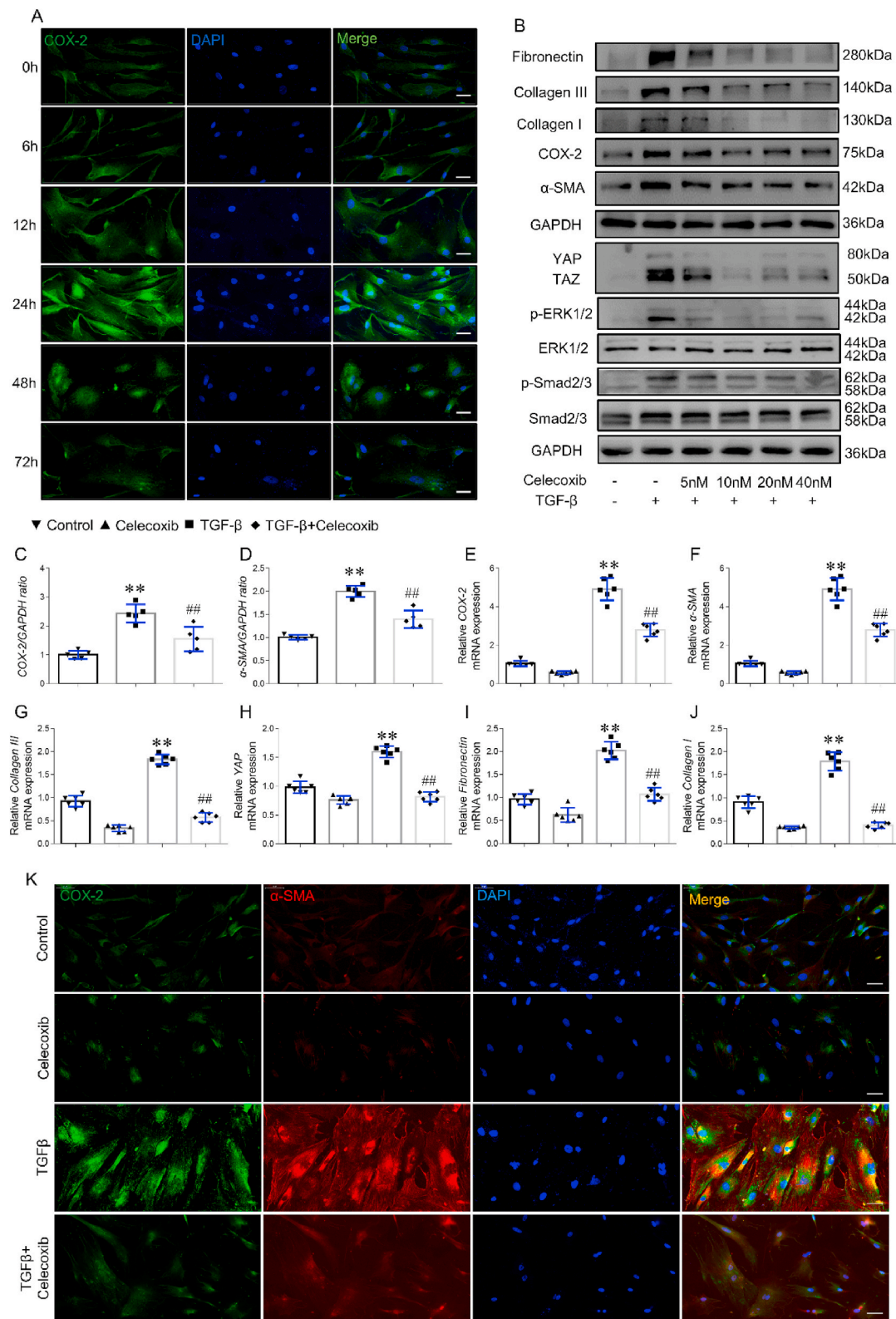


Fig. 2. Celecoxib inhibits myfibroblast differentiation and fibrosis by inhibiting canonical and non-canonical TGF-β signaling pathways. (A) Representative images showing COX-2 staining of TGF-β-stimulated fibroblasts in time dependent manner. Scale bar = 40 μm. (B) Representative immunoblot showing expression levels of α-SMA, YAP-TAZ, collagen I, collagen III, fibronectin, COX-2 Smad2/3, p-Smad2/3, ERK1/2 and p- ERK1/2 in fibroblasts pre-treated with celecoxib for different concentrations after TGF-β stimulation. (C, D) Quantitative analysis of COX-2 and α-SMA expression treated with TGF-β or celecoxib (10 nM). (E–J) Relative COX-2 (E), α-SMA (F), collagen III (G), YAP (H), fibronectin (I) and collagen I (J) mRNA levels in the suitably treated fibroblasts (n = 6). **p < 0.01, compared to the control group. ##p < 0.01, compared to the TGF-β group. (K) Immunofluorescence analysis of α-SMA and COX-2 expression in TGF-β-cultured fibroblasts treated with 10 nM celecoxib for 24 h. α-SMA (green), COX-2 (red) and DAPI (blue) are shown in representative immunofluorescence microscopic images. Scale bar = 50 μm.

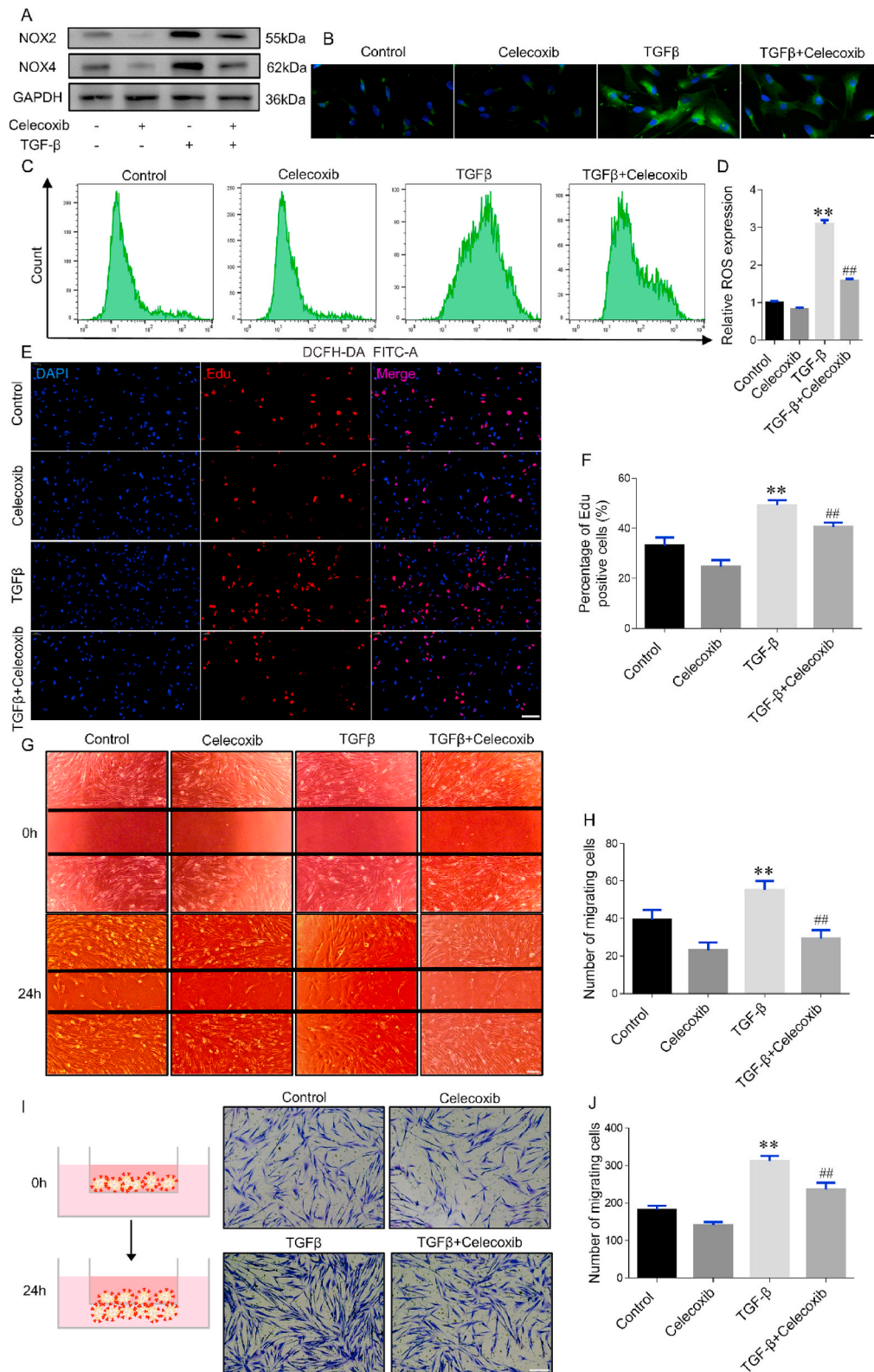


Fig. 3. Celecoxib inhibited oxidative stress and fibroblast proliferation and migration. (A) Representative immunoblot showing expression levels of NOX2 and NOX4 in fibroblasts pre-treated with celecoxib or TGF-β stimulation. (B) DCFH-DA staining of ROS after fibroblasts was treated with celecoxib or TGF-β. Scale bar = 20 μm. (C) Flow cytometry and analysis of ROS fluorescent cells. (D) Quantitative analysis of ROS expression (E) Edu analysis showing proliferative fibroblasts after celecoxib or TGF-β treatment. Scale bar = 100 μm. (F) Quantitative analysis of proliferative cells in control, celecoxib, TGF-β, TGF-β+celecoxib groups. (G) Representative images of wound-healing assay at 0 and 24h. Scale bar = 10 μm. (H) Quantitative analysis of number of migrating cells into the gap. (I) Representative images of transwell assay with fibroblasts treated as indicated. Scale bar = 100 μm. (J) Quantitative analysis of number of cells migrating across the membrane. Data represent mean ± SD of 6 independent experiments. ***p* < 0.01, compared to the control group. ##*p* < 0.01, compared to the TGF-β group.

2.4. Pharmacological inhibition of COX-2 showed potent antifibrotic effects for the improvement of muscle preservation

Since our *in vitro* findings showed anti-fibrosis effect of celecoxib, their characteristics during fibrogenesis were further explored *in vivo*. We sought to determine whether suppression of COX-2 caused by celecoxib was able to ameliorate skeletal muscle atrophy induced by surgery during the fibrotic stage. As shown in Fig. 4A, celecoxib was administered p.o. every 24 h after skeletal muscle injury. Fibrosis initiation did not cease or regress even after surgical injury was terminated and showed a self-sustaining ability. The restoration process of skeletal muscle degeneration is characterized by high levels of collagen formation and muscle atrophy. In the present study, examination of histological sections of injured skeletal muscle demonstrated the progression of skeletal muscle deterioration due to replacement of fibrous scars with collagen deposition, while in uninjured skeletal muscles, collagen fiber was undetectable. The levels of muscle degeneration significantly increased from 3 days to 28 days after injury and the fibrotic areas had grown larger as time went by (Fig. 4B–G). Selective inhibition of COX-2 by celecoxib significantly reduced the severity of muscle deterioration as a result of significantly decreased levels of scar formation and skeletal muscle atrophy at different time points after injury (Fig. 4H–L). We also found that injured tissues of mice treated with celecoxib displayed decreased levels of COX-2 expression (Fig. 4M). Importantly, immunofluorescence analysis suggested that increased α -SMA, collagen I, fibronectin and YAP/TAZ positive areas were distributed throughout the fibrotic regions of injured muscles, compared with the control group and *in vivo* treatment of celecoxib significantly decreased the expression of these genes expression (Fig. 4M). Consistent with the results of the *in vitro* experiments, injured tissues from the celecoxib-treated mice demonstrated significantly decreased levels of expression of mRNA encoding the fibrosis-associated genes (Fig. 4N–R).

2.5. Celecoxib weakened profibrotic kinase pathways and oxidative stress *in vivo*

Given that myofibroblasts secrete collagen in an extracellular ERK-dependent pathway and that TGF- β signaling pathway plays a crucial role in fibrogenesis, we first evaluated whether celecoxib could decrease phosphorylation of ERK1/2 and Smad2/3. We found that phosphorylation of Smad2/3, ERK1/2 and TGF- β R1 were significantly increased in injured muscle tissues (Fig. 5J–M) compared to control group (Fig. 5A–D). Similarly, celecoxib markedly decreased p-Smad2/3, p-ERK1/2 and TGF- β R1 positive areas (Fig. 5S–V). Western blotting analysis further confirmed that the inhibition of COX-2 expression weakened these profibrotic kinase pathways *in vivo* (Fig. 5BB and CC). Angiogenesis is a process by which new blood vessels are formed. During this process, vascular endothelial growth factor (VEGF) acts as a positive key regulator of fibrogenesis. We found that celecoxib could decrease the expression levels of VEGF *in vivo*, compared to injury group (Fig. 5E, N, W and CC) and reduced VEGF expression in supernatant of fibroblasts after TGF- β treatment (Fig. 5DD). Besides, celecoxib also significantly inhibited oxidative stress by decreasing the level of NOX2 and NOX4 compared to injury group (Fig. 5P–R, Y-AA, CC).

2.6. COX-2 regulated multiple genes by wide-range interactions

We employed RNA-seq to further explore the regulatory elements by COX-2. RNA-seq analysis indicated significant changes in mRNA after COX-2 was inhibited (Fig. 6A). The transcriptomic study implicated 101 differentially expressed genes (DEGs) in the three TGF- β groups compared to the TGF- β +celecoxib groups, including 58 up-regulated and 43 down-regulated genes (Fig. 6B and C). By GO annotation, the enrichment trends of differentially expressed genes were found in pre-synaptic process involved in chemical synaptic transmission, detoxification and cell killing of biological process; virion part, nucleoid part

and other organism part of cellular component; signal transducer activity, molecular transducer activity, electron carrier activity, antioxidant activity and translation regulator activity of molecular function (Fig. 6D). Moreover, PDK1 was significantly altered in PI3K-AKT pathway after celecoxib treatment (Fig. 54). Reportedly, PDK1/AKT pathway is associated with fibrogenesis [60] and complex regulatory networks by COX-2 still requires further investigations.

2.7. Knockdown of COX-2 inhibited AKT activation by reducing PDK1 expression and E3 ubiquitin ligase TRAF4 recruitment

To further confirm the relationship between COX-2, PDK1 and its downstream AKT signaling, we first explored the colocalization of COX-2 and PDK1 by immunofluorescence methods (Fig. 7A). Pearson's for image above thresholds was 0.8489 (Fig. 7B) and co-located plot profile image was shown in Fig. 7C. Then we detected the PDK1/AKT components in the COX-2 associated CO-IP complex. The results of immunoprecipitation analysis indicated that COX-2 interacted with PDK1 and AKT (Fig. 7D and E). Inhibition or overexpression of COX-2 by siRNA or rebamipide was confirmed by RT-PCR (Fig. 7F) and we observed that si-COX-2 could significantly decrease the level of PDK1 while overexpression of COX-2 markedly increased PDK1 content (Fig. 7G). Both Pharmacological or genetic inactivation of COX-2 inhibited the expression of PDK1 and subsequently suppressed phosphorylation of AKT (Fig. 7H). Besides, previous studies indicated that TRAF4 of E3 ligases activated AKT by facilitating its K63-linked ubiquitination [49]. Both TGF- β and oe-COX-2 could promote the association between TRAF4 and AKT, which was blocked by si-COX-2 (Fig. 7I). Immunoprecipitation analysis further confirmed the inhibitory effect of si-COX-2 on Lys63 polyubiquitination of AKT in fibroblasts cultured with TGF- β (Fig. 7J). Overall, we demonstrated that knockdown of COX-2 inhibited TGF- β induced AKT activation by suppressing its upstream signaling PDK1 and blocking the interaction between TRAF4 and AKT and the subsequent Lys63 polyubiquitination of AKT.

3. Discussion

Skeletal muscle atrophy can significantly delay recovery of motor function, extend hospital stay and increase morbidity and mortality. However, the molecular mechanism underlying its occurrence and development remains unclear [61,62]. Considering its extensive clinical implications, pharmacological therapies are desperately indispensable. In the present study, we focused on the preservation of resident of skeletal muscle fibers and the reduction of myofibroblasts accumulation and collagen deposition by pharmacological or genetic inactivation of COX-2.

NSAIDs (nonselective or selective COX-2 inhibitor like celecoxib) are predominantly used as analgesics to manage postoperative pain worldwide [33,35,63]. Only a few studies have evaluated the effect of celecoxib on skeletal muscle fibrosis. The role of celecoxib in various types of fibrogenesis remains controversial. Administration of celecoxib prevents tendon fibrosis [44] and reduces peritoneal fibrosis [64], as well as ameliorates cystic fibrosis [65], whereas, on the other hand, the inhibition of COX-2-derived PGE2 after celecoxib treatment may accelerate the progression of fibrosis [66]. It is well known that COX is a limited enzyme in the synthesis process of converting arachidonic acid into prostaglandin H2 and further conversion of the product into prostaglandins, such as PGD2 and PGE2. Exogenous PGD2 and PGE2 exert a strong inhibitory effect on fibroblast proliferation and differentiation. We found that levels of PGD2 and PGE2 decreased after celecoxib promoted dedifferentiation (Fig. S2A–C), while both exogenous PGD2 and PGE2 inhibited the expression of α -SMA and collagen I. Interestingly, celecoxib decreased PGD2 and PGE2 expression in fibroblasts, while inhibiting TGF- β -induced myofibroblast activation and collagen deposition, instead of severe fibrosis. These results indicated that the potential cellular mechanism of COX-2 in fibrogenesis has not been fully

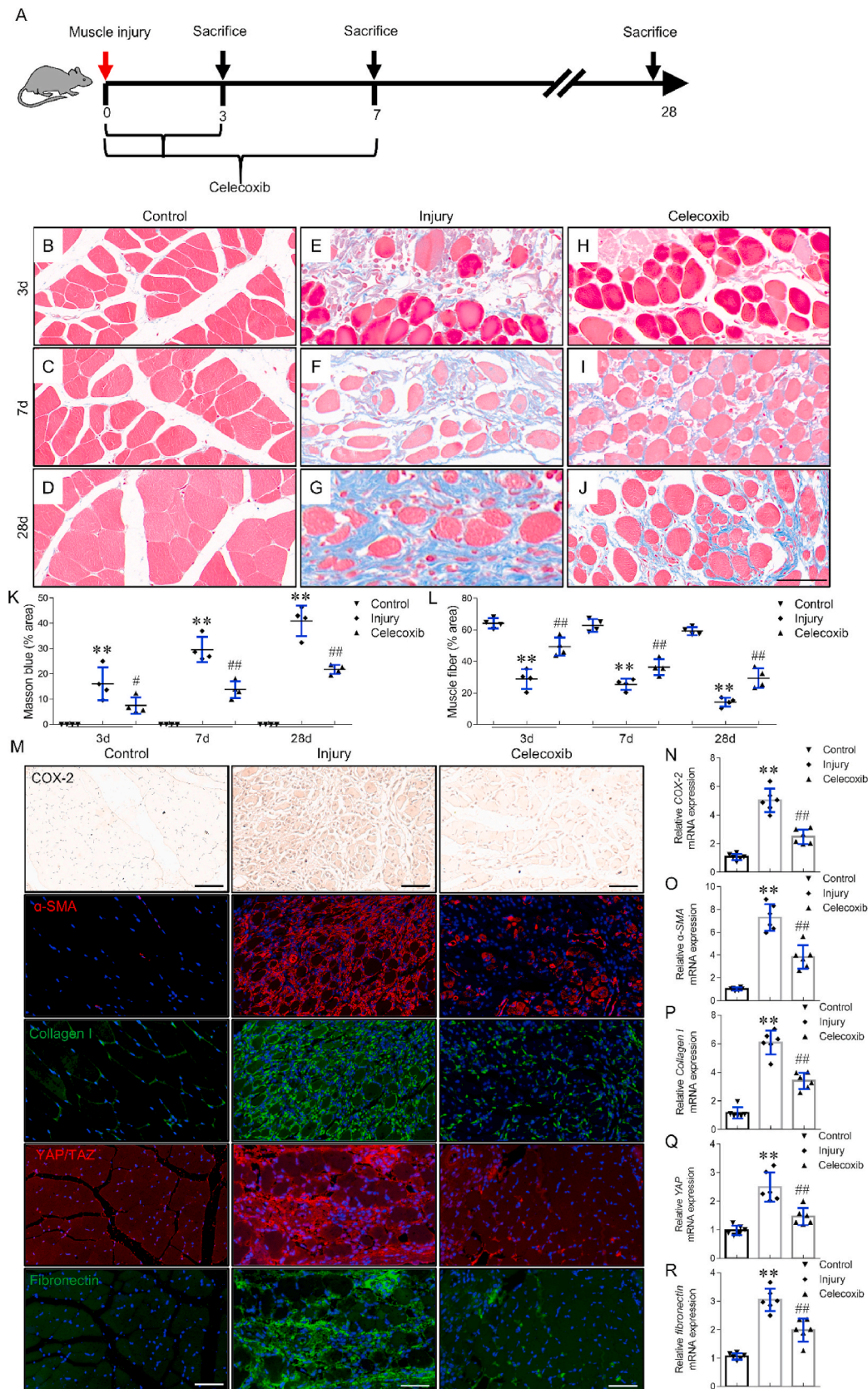


Fig. 4. Inhibition of COX-2 suppresses fibrosis and alleviates skeletal muscle atrophy. (A) Treatment regimen for skeletal muscle injury mouse model. (B–J) Representative images of Masson stained skeletal muscle tissues from the control (B–D), injury (E–G) and celecoxib (H–J) groups at different time points after surgery-induced injury. Scale bar = 50 μ m. Percentage of collagen (K) and muscle fibers (L) in the indicated groups. (M) Representative images of muscle tissues immunostained for COX-2, α -SMA, collagen I, YAP and fibronectin. Scale bar = 50 μ m. (N–R) Relative mRNA expression levels of fibrotic markers in the indicated groups. Each symbol represents an individual mouse (n = 6). ** p < 0.01, compared to the control group. ## p < 0.01, compared to the injury group.

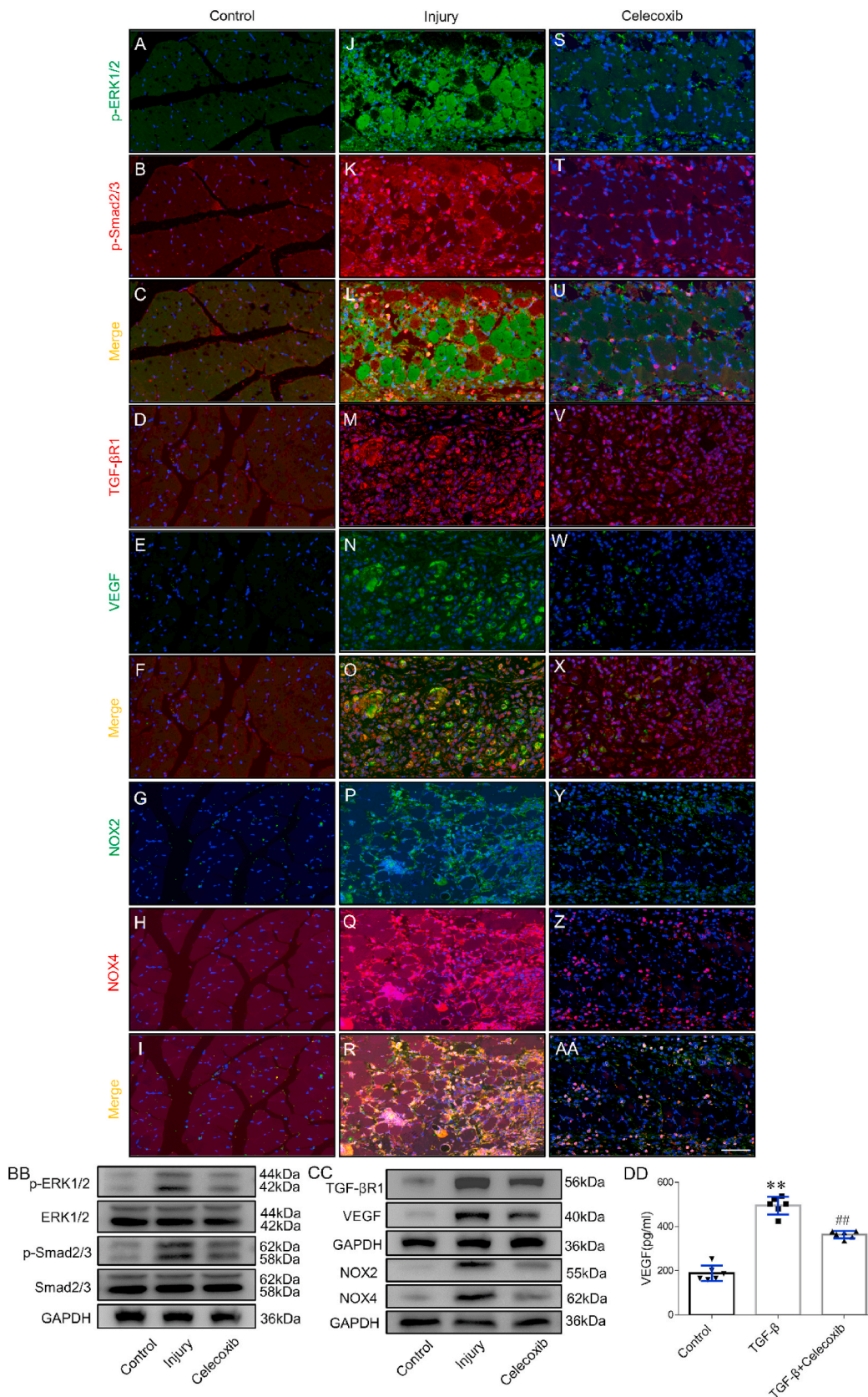


Fig. 5. Celecoxib weakened oxidative stress and profibrotic kinase pathways *in vivo*. Representative images of p-ERK1/2, TGF-βR1, p-Smad2/3, VEGF, NOX2 and NOX4 immunostaining in injured muscles of the control (A–I), injury (J–R) and celecoxib (S–AA) groups. Scale bar = 50 μm. (BB) Immunoblot showing p-ERK1/2 and p-Smad2/3 levels in the muscles of indicated groups. (CC) Immunoblot showing TGF-βR1, VEGF, NOX2 and NOX4 levels in the muscles of indicated groups. (DD) VEGF levels in the supernatant of fibroblasts treated with celecoxib before TGF-β stimulation (n = 6). ***p* < 0.01, compared to the control group. ##*p* < 0.01, compared to the TGF-β group.

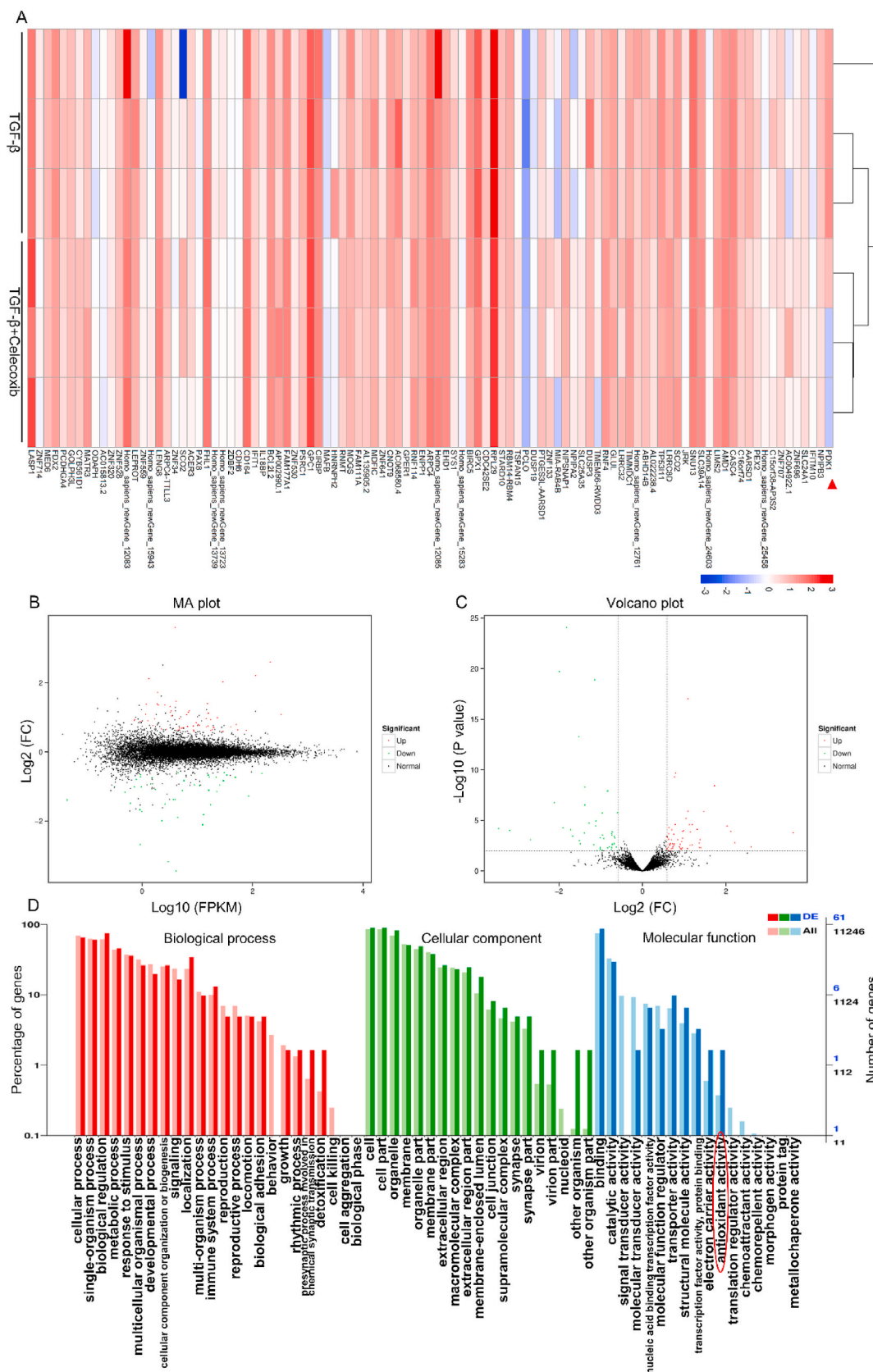


Fig. 6. COX-2 interacted with multiple genes. (A) A heat map showed differentially expressed genes (DEGs) in TGF-β activated fibroblasts that were pretreated with celecoxib or not. (B) The MA diagram provided an intuitive view of the overall distribution of expression levels and differential multiples of two groups of genes. (C) Volcano Plot displayed DEGs between two groups. (D) Based on DEGs and all genes, the enrichment of the secondary functions of GO reflected the status of the secondary functions in the two backgrounds and antioxidant activity was involved (indicated by red circle). (For interpretation of the references to color in this figure legend, the reader is referred to the Web version of this article.)

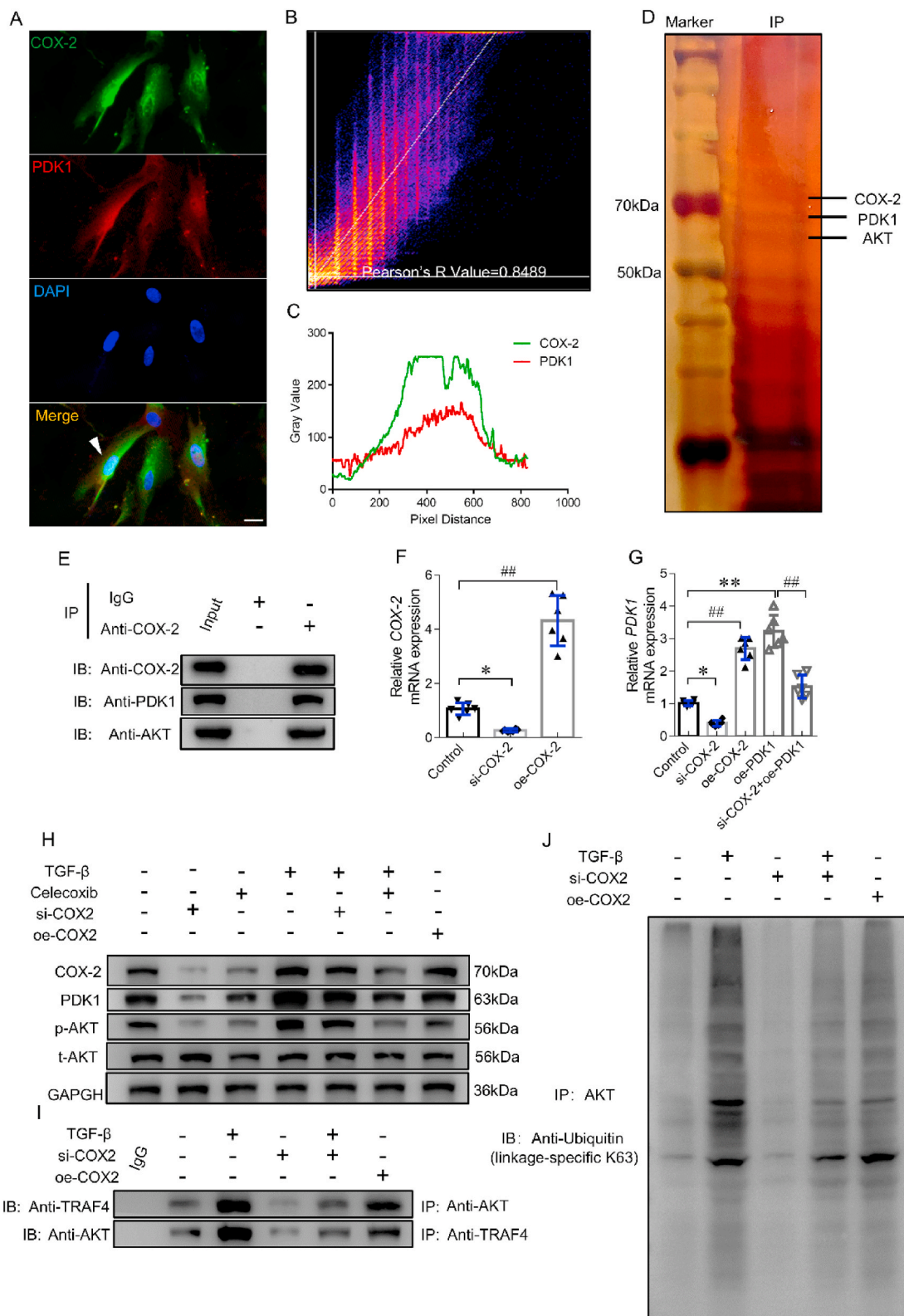


Fig. 7. Knockdown of COX-2 inhibited PDK1 expression and E3 ubiquitin ligase TRAF4 recruitment to suppress AKT activation. (A) The colocalization of COX-2 and PDK1 was evaluated by immunofluorescence. Scale bar = 20 μ m (B) Co-localization analysis was shown by scatter plot of all fibroblasts. (C) Plot profile image displayed colocalization of the fibroblasts indicated by the white arrow. (D) Co-immunoprecipitation and silver staining analysis of COX-2 associated proteins in fibroblasts. (E) Co-immunoprecipitation analyses of the interaction between COX-2, PDK1 and AKT in fibroblasts. (F) mRNA of COX-2 was detected after knockdown by COX-2 si-RNA or overexpression by rebamipide. (G) mRNA of PDK1 was measured after gain or loss of COX-2. (H) Western blotting analysis was utilized to measure COX-2, PDK1 and *p*-AKT expression levels in fibroblasts after suitable treatment. (I) Co-immunoprecipitation assays were done to confirm the interaction between TRAF4 and AKT. (J) Immunoprecipitation was then conducted to detect the effect of COX-2 on the expression of Lys63-polyubiquitination of AKT.

elucidated.

COX-2 has been widely investigated in cancer and it is especially intriguing that activated fibroblasts and cancer cells show numerous similarities in phenotype and share a gene-expression pattern. COX-2 is highly expressed in various tumors, including breast [67], lung [68], prostate [69], and colorectal cancers [70]. We found that COX-2 expression was remarkably higher in the muscle injury site caused by bone fracture as opposed to normal regions muscles of both humans and mice that had been affected by surgery-induced muscle injury, compared to non-damaged muscles. It has been reported that the morphological structures of the fibroblastic foci are heterogeneous and can be divided into two different regions: the active fibrotic front and the myofibroblast core, based on content and size, positioning the active fibrotic front as a temporal growth of the fibroblastic foci that can invade into adjacent normal skeletal muscle tissue and the myofibroblast core, as a source of collagen deposition and fibronectin production [51]. As shown in the present study, the results of our immunohistochemical studies characterized the active fibrotic front using the expression of Ki67 and S100A10, the markers of mesenchymal progenitor cell. Besides, COX-2 was also significantly increased in the in the high cellular density region, indicating that COX-2 positive cells are crucial components of the active fibrotic front in the fibroblastic foci.

It is important that fibroblasts differentiate into myofibroblasts since this process produces collagen deposition for repair of the injury site. In parallel experiments performed *in vitro*, COX-2 expression increased when fibroblasts were activated but decreased as fibroblasts matured into myofibroblasts. The use of celecoxib to pharmacologically interfere with COX-2 levels simultaneously promoted myofibroblast dedifferentiation and inhibited ECM formation, as reflected by the downregulation of α -SMA and other fibrosis related genes (collagen I, collagen III and fibronectin) (Fig. 8). Our results linked the upregulation of COX-2 expression with myofibroblast differentiation and the mechanism by which COX-2 expression promoted differentiation remains to be examined further. The YAP-TAZ and phosphorylation of Smad2/3 and ERK1/2 induced by additional TGF- β expression was shown to aggravate the fibrosis response [71,72]. Since celecoxib could partially reverse TGF- β induced myofibroblast differentiation, the underlying mechanisms need to be investigated further. Celecoxib caused downregulation of YAP-TAZ, phosphorylated Smad2/3 and ERK1/2 expression after TGF- β

treatment. Fibroblasts undergo remarkable alteration in phenotype and gene expression, which results in cell proliferation and migration. We found that inactivation of COX-2 could suppress fibroblast proliferation and migration induced by TGF- β .

We sought to explore the contribution of celecoxib towards fibrogenesis *in vivo* using a skeletal muscle injury mouse model. In accordance with the *ex vivo* analysis, the *in vivo* results revealed that inactivation of COX-2 resulted in the dedifferentiation of myofibroblasts and decreased ECM levels of α -SMA, collagen, and fibronectin content. Celecoxib interfered with TGF- β /SMAD signaling through the inhibition of TGF- β R1 expression and the phosphorylation of Smad2/3. Non-canonical TGF β pathways, such as YAP of Hippo, ERK1/2 of MAPK signaling, as well as VEGF were also mediated by inhibition of COX-2 in the skeletal muscle fibrosis mouse model. In addition, inhibition of COX-2 relieved oxidative stress and ROS generation. These results indicate that the overexpression of COX-2 confers fibroblasts with fibrogenic properties that result in collagen deposition and ECM products. Our results demonstrated that the administration of celecoxib exert anti-fibrosis effects on fibrosis and that the pharmacological inhibition of COX-2 expression was sufficient to provide remarkable protection against fibrosis at all the fibrotic end points detected.

We further investigate other pathways that are involved in skeletal muscle fibrosis by RNA-seq. In the present study, we found celecoxib could significantly inhibit the expression of PDK1 and PDK1/AKT signaling was previously to be closely associated with fibrosis [60]. We demonstrated that COX-2 could interact with PDK1 and AKT and knockdown of COX-2 could significantly inhibit the PDK1 expression and subsequently suppress the phosphorylation of AKT. In addition, we observed that inhibition of COX-2 decreased the TGF- β mediated K63 ubiquitination of AKT by suppressing the interaction between TRAF4 and AKT. On the contrary, overexpression of COX-2 was found to reverse this effect.

In conclusion, we identified COX-2 as a promoter of fibroblast proliferation, differentiation and migration and showed that COX-2 positive cells are crucial components of the active fibrotic front in the fibroblastic foci. Inactivation of COX-2 showed potent anti-fibrotic properties by inhibiting canonical and non-canonical TGF- β signaling pathways. In general, based on the results of this study, controlling COX-2 expression might be available treatment of skeletal muscle atrophy in the future.

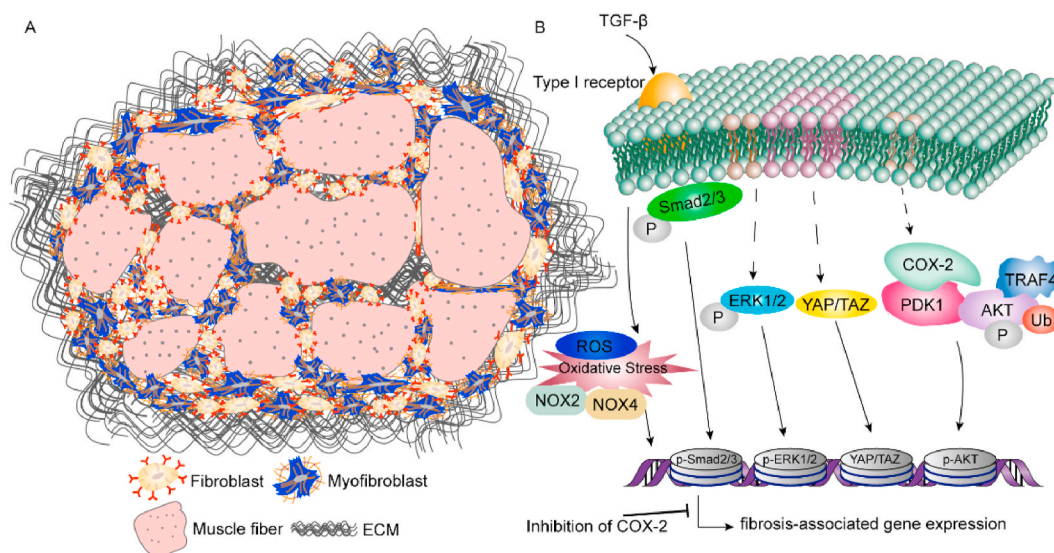


Fig. 8. Schematic representation of fibrogenesis during skeletal muscle atrophy. (A) After skeletal muscle injury, resident fibroblasts or migrated from peripheral region proliferated and differentiated into myofibroblasts to produce ECM. Mass collagen deposition replaced skeletal muscle regeneration and induced atrophy. (B) Skeletal muscle injury induced release of various cytokines activated TGF- β -dependent signaling pathway, non-canonical TGF- β pathways and oxidative stress. COX-2 promoted AKT activation by increasing its upstream signaling PDK1 and facilitating the interaction between TRAF4 and AKT and the subsequent Lys63 poly-ubiquitination of AKT. Inhibition of COX-2 showed significant inhibitory effect on the signaling pathway that were positive for fibrogenesis.

4. Materials and methods

4.1. Tissue specimens and cell culture

Injured muscle tissues surrounding bone fractures and normal muscle specimens were resected from 6 patients (Table S1) admitted to the Department of Orthopedics at the First Affiliated Hospital of Nanjing Medical University of China. To isolate primary fibroblasts, the injured muscle tissues were separated into hair-like strands (5 mm × 5 mm) by soaking in 75% alcohol for 10 min. After incubating the muscle strands with trypsin-EDTA (Keygen, Nanjing, China) for 5 min at 37 °C, the digested tissue masses were centrifuged at 1300 rpm for 5 min. The extracted fibroblasts were seeded in 25 cm² culture flasks in Dulbecco's modified Eagle medium (DMEM, Gibco) supplemented with 10% fetal bovine serum (FBS, Gibco) and 1% penicillin/streptomycin (Gibco), and cultured at 37 °C under 5% CO₂.

4.2. Cell treatment and transfections

The fibroblasts from passages 3 and 5 were activated with 10 ng/ml transforming growth factor-beta (TGF-β, BioLegend) following a 24h pre-treatment with 5, 10, 20 and 40 nM celecoxib (Abcam). COX-2 siRNA (Santa Cruz Biotechnology, TX, USA) was used to transfect fibroblasts using DharmaFECT 1 transfection reagent based on the manufacturer's protocol. In brief, Serum-free medium was added to cells 1 h before transfection. A total of 100 μl COX-2 siRNA and 40 μl transfection reagents were diluted in 2 ml separate serum-free medium and incubated at room temperature for 15 min. Then the mixture was added to the 10% DMEM to get the final concentration of 50 nM. After 24 h of incubation, the medium containing the COX-2 siRNA was replaced by siRNA free culture. Rebamipide (MedChemExpress) at the concentration of 10 nM was used to overexpress COX-2 level. 5 μM PDK1 activator PS48 (MedChemExpress) was employed to overexpress PDK1.

4.3. Establishment of muscle injury model

Male C57BL/6J mice aged 6–8 weeks and weighing 20–25g were obtained from Experimental Animal Center of Nanjing Medical University, Nanjing, China. The mice were housed at 25 ± 1 °C, relative humidity 60 ± 10%, and 12h/12h light and dark cycle, and provided with food and water ad libitum. To induce muscle injury, the mice were first anesthetized by intraperitoneal injection of ketamine and xylazine, and placed on the console in a prone position. The dorsal region was depilated, and the skin was disinfected with iodophor and incised. The underlying fascia was separated, and the latissimus dorsi muscle was cut through. After the injured muscle was flushed with saline, and the wound was sutured layer by layer, followed by disinfection of the skin. The mice were randomly divided into the control, injury and celecoxib groups. Mice in control group underwent no surgery and in injury or celecoxib group, mice were intra-gastrically infused with 0.9% NaCl, or 100 mg/kg celecoxib [73] (dissolved in normal saline) respectively (Qd for 3 or 7 days after operation) after surgery.

4.4. Real-time polymerase chain reaction (RT-PCR)

Total RNA was extracted from the cultured cells using Trizol reagent according to the manufacturer's instructions, and reverse transcribed to cDNA using Prime Script TM Master Mix (Takara). The RT-PCR was performed using the SYBR Green Mix (Vazyme Biotech) and the following primers (Table S2). The relative gene expression levels were calculated with the 2^{-ΔΔCt} formula with GAPDH as the internal control.

4.5. Western blotting and immunoprecipitation

Protein was extracted from the suitably treated fibroblasts using the Whole Cell Lysis Kit (Keygen, Nanjing, China). The lysate was

centrifuged for 15 min at 4 °C and 12000 rpm, and the protein content in the supernatant was analyzed by the Bradford method. Equal amount of proteins per sample were resolved by SDS-PAGE using a 10% separating gel, and transferred into polyvinylidene fluoride (PVDF) membranes. After blocking with 5% skim milk in tris-buffered saline with Tween-20 (TBST) at room temperature for 1h, the membranes were washed thrice with TBST (5min each time). The blots were then incubated overnight at 4 °C with primary antibodies against YAP/TAZ (#8418S), Smad2/3 (#12470S), p-Smad2/3 (#8828S), Erk1/2 (#4695P), p-Erk1/2 (#4370S), p-P38 (#4511S), AKT (#4685), p-AKT (#13038) (all from Cell Signaling Technologies), α-SMA (#ab5694), COX-2 (#ab15191), collagen I (#ab34710), fibronectin (#ab6328), P38 (#ab31828) and TRAF4 (#ab245666) (all from Abcam), collagen III (#13548-1-AP), NOX2 (#19013-1-AP), NOX4 (#14347-1-AP) and GAPDH (#HRP-60004) (Proteintech). The anti-GAPDH antibody was diluted 1:10000, and the other antibodies were diluted 1:1000. After washing thrice with TBST (10min each time), the blots were incubated with goat-anti-rabbit IgG (#YFSA02) or goat-anti-mouse IgG (#YFSA01) (YiFeiXue Biotech) at room temperature for 1h. The blots were washed again, and the bands were visualized by electrochemiluminescence (ECL). The western bands were quantified using Image J software.

Immunoprecipitation analysis was conducted according to previously study [74]. Briefly, proteins from the treated fibroblasts was mixed with COX-2, AKT or TRAF4 antibody at 4 °C overnight. Protein A/G agarose beads (Invitrogen, USA) was then used to incubate the mixture at 4 °C for 4 h and the final product was analyzed by Western blot.

4.6. Immunofluorescence

The suitably treated fibroblasts were seeded into 12-well plates (WHB, Shanghai, China) and cultured till the desired confluency. The cells were then washed with PBS and fixed with 4% paraformaldehyde (PFA) (Servicebio, Wuhan, China) for 20min. After washing thrice with PBS (3min each time), the cells were permeabilized with 0.5% Triton X-100 (Biofroxx), and then blocked with serum (Beyotime) homologous to the secondary antibody for 30 min. The serum was discarded, and the cells were incubated overnight with the suitable antibodies at 4 °C. Following a PBS wash, the cells were incubated with Alexa Fluor 488goat anti-rabbit IgG (1:500; #136832, Jackson) and Alexa Fluor 568 donkey anti-rabbit IgG (1:500; #A10042, Invitrogen) at 37 °C for 30min in the dark. Finally, the cells were washed with PBS, counterstained with DAPI Fluoromount-G (Southernbiotech), and observed under a fluorescence microscope.

Measurement of colocalization areas was conducted using ImageJ software. Colocalization analysis was done by Image J plugins JaCop, Colocalization colormap and Colocalization threshold according to a previous study [75].

4.7. Immunohistochemistry

Muscles were resected from the suitably treated mice and fixed in 4% PFA for 24h. After routine decalcification and dehydration through an ethanol gradient, the tissues were embedded in paraffin and cut into 3 μm sections using a rotary microtome. The sections were cleared with xylene and ethanol, and immersed in boiling citrate buffer (pH 6) for 25 min for antigen retrieval. After blocking with BSA for an hour at room temperature, the muscle sections were incubated overnight with primary antibodies against YAP/TAZ (1:500), fibronectin (1:500), COX-2 (1:1000), collagen I (1:500), α-SMA (1:100), Ki67 (1:200, #GB13030-2), S100A4 (1:200, #GB12397), CD68 (1:200, #GB11067) (all from Servicebio) at 4 °C. The sections were washed to remove the primary antibodies, and then probed with goat-anti-rabbit IgG (#GB23303) and goat-anti-mouse IgG (#GB23301) secondary antibodies (diluted 1:500, Servicebio) for 50 min, followed by CY3, FITC or CY5 (Servicebio) for 10 min in the dark. After washing with TBST, the sections were counterstained with DAPI Fluoromount-G and observed under a fluorescence

microscope.

Muscle tissues were sliced into 3 μm sections as per standard protocols. Following deparaffinization and dehydration as described above, the sections were immersed in EDTA antigen retrieval buffer (pH 8; Servicebio) and boiled for 30 min. The sections were blocked with BSA for 30 min, and then incubated overnight with *anti*-COX-2 antibody (1:100) at 4 °C, followed by MaxVision™ HRP-Polymer anti-rabbit antibody (MXB) and Vectastain ABC Kit (Vector) according to the manufacturer's protocol. The color was developed using DAB (Vector) and hematoxylin (Servicebio) was used to counterstain for 30s. After a final wash with PBS, the sections were cleared with 1% ethanol hydrochloride, dehydrated, and observed under a microscope.

4.8. Histological examination

The muscle sections were processed as described above, and stained with hematoxylin-eosin (HE) for histopathological examination. Masson Trichrome staining was also performed as per standard protocols to analyze fiber deposition.

4.9. Cell proliferation assay

The fibroblasts were seeded into a 96-well plate (WHB) at the density of 1×10^4 /well. After treating the cells with celecoxib or TGF- β for 24h, a kFluor555-EdU kit (Keygen Biotech, Nanjing, China) was used to evaluate the proliferative ability of fibroblasts. Briefly, 10% DMEM containing Edu (10 μM) was used to incubate cells for 72h, 4% paraformaldehyde was employed to fix cells for 15min and DAPI staining was then performed.

4.10. Transwell and wound-healing assays

Fibroblasts were seeded into the upper chambers of transwell inserts (8 μm membrane pore size; Corning) in a 24-well plate (WHB) in serum-free medium with the respective drugs at the density of 2×10^5 cells/well, and the lower chambers were filled with 500 μl complete DMEM containing TGF- β . After culturing for 24h, the inserts were removed and unigrated cells on the upper surface of the membrane were wiped with a cotton swab. The migrated cells on the lower surface were fixed with 4% PFA for 30 min and stained with 0.1% crystal violet for 30min, and counted under a microscope. For wound-healing assay, fibroblasts were seeded into 4-well inserts (Ibidi) in a 12-well plate (WHB, Shanghai, China) and grown till confluent. The monolayer was scratched with a sterile pipette tip, and fresh medium containing TGF- β or celecoxib was added. The wound area was photographed at 0h and 24h.

4.11. Detection of ROS

Fibroblasts treated by celecoxib or TGF- β were washed in PBS for 3 times for 5 min. DCFH-DA (Keygen, Nanjing, China) was used to incubate cells at 10 μM for 1 h at 37 °C in dark. Incubation buffer was removed and DMEM-F12 was then employed to incubate cells for 30 min. Fibroblasts were observed by fluorescence microscope. For flow-cytometry analysis, the fibroblasts were obtained for suspension in DMEM-F12 and washed with PBS for 3 times for 5 min. ROS was detected at a wavelength of 488 nm.

4.12. RNA-seq analysis

Total RNA was extracted from TGF- β -activated fibroblasts pretreated with celecoxib or not by TRIzol reagent according to the manufacturer's protocol. The RNA-seq prepared libraries were sequenced using an Illumina HiSeq 4000 sequencer (Biomarker Technologies, Beijing, China) after ribosomal RNA was eliminated. As described previously [76], the gene expression levels were measured by Tophat and Cufflinks. Enrichment analysis for the biological processes, molecular function and

cellular component were done on the basis of the GO database annotations with DAVID. Differentially expressed gene pathways were annotated by KEGG (Kyoto Encyclopedia of Genes and Genomes). Fusionmap was used to investigate gene fusion events in the transcriptome. Fold Change ≥ 1.5 and P-value < 0.01 were used as screening criteria in the detection of differentially expressed genes.

4.13. Statistical analysis

Data are expressed as the mean \pm SD of three independent experiments. Two-tailed *t*-test and one-way ANOVA followed by post hoc Bonferroni's correction were respectively used to compare two and multiple groups. Statistical analysis was performed with GraphPad Prism 6 software. *P* < 0.05 was considered statistically significant.

4.14. Study approval

All patients provided informed consent, and the Ethic Committee of the First Affiliated Hospital of Nanjing Medical University approved the study according to the Declaration of Helsinki (No. 2010-SR-088). Animal experiments were approved by the Institutional Animal Care and Use Committee (IACUC) of Nanjing Medical University, China (Approval No.: IACUC-1710004) and in conformity with the Guide for the Care and Use of Laboratory Animals (National Academies Press, 2011).

Author contributions

HC, ZQ, SZ, and XC conceived and designed the experiments. HC, JT, LF, DG, JC, FJ, JC and LY collected, analyzed and interpreted the data. HC and XC drafted the article.

Declaration of competing interest

The authors declare that they have no conflict of interest.

Acknowledgments

This work was supported by grants from the National Natural Science Foundation of China (81871773, 81672152 to XC; 81802149 to LY), Natural Science Foundation of Jiangsu Province (BK20171089 to JT) and Primary Research and Development Plan of Jiangsu Province (BE2018132 to XC).

Appendix A. Supplementary data

Supplementary data to this article can be found online at <https://doi.org/10.1016/j.redox.2020.101774>.

References

- [1] M.C. Gomez-Cabrera, C. Arc-Chagnaud, A. Salvador-Pascual, et al., Redox modulation of muscle mass and function, *Redox Biol* 35 (2020) 101531.
- [2] R. Valle-Tenney, D.L. Rebolledo, K.E. Lipson, et al., Role of hypoxia in skeletal muscle fibrosis: synergism between hypoxia and TGF-beta signaling upregulates CCN2/CTGF expression specifically in muscle fibers, *Matrix Biol.* 87 (2020) 48–65.
- [3] D.L. Rebolledo, D. González, J. Faundez-Contreras, et al., Denervation-induced skeletal muscle fibrosis is mediated by CTGF/CCN2 independently of TGF- β , *Matrix Biol.* 82 (2019) 20–37.
- [4] S.M. Ebert, A. Al-Zougbi, S.C. Bodine, et al., Skeletal muscle atrophy: discovery of mechanisms and potential therapies, *Physiology* 34 (2019) 232–239.
- [5] V. Vogel, Unraveling the mechanobiology of extracellular matrix, *Annu. Rev. Physiol.* 80 (2018) 353–387.
- [6] J. Herrera, C.A. Henke, P.B. Bitterman, Extracellular matrix as a driver of progressive fibrosis, *J. Clin. Invest.* 128 (2018) 45–53.
- [7] L. Madaro, M. Passafaro, D. Sala, et al., Denervation-activated STAT3-IL-6 signalling in fibro-adipogenic progenitors promotes myofibres atrophy and fibrosis, *Nat. Cell Biol.* 20 (2018) 917–927.
- [8] N. Horii, M. Uchida, N. Hasegawa, et al., Resistance training prevents muscle fibrosis and atrophy via down-regulation of C1q-induced Wnt signaling in senescent mice, *Faseb. J.* 32 (2018) 3547–3559.

- [9] P. Zhang, J. He, F. Wang, et al., Hemojuvelin is a novel suppressor for Duchenne muscular dystrophy and age-related muscle wasting, *J Cachexia Sarcopenia Muscle* 10 (2019) 557–573.
- [10] P. Harish, A. Malerba, N. Lu-Nguyen, et al., Inhibition of myostatin improves muscle atrophy in oculopharyngeal muscular dystrophy (OPMD), *J Cachexia Sarcopenia Muscle* 10 (2019) 1016–1026.
- [11] D.J. Tschumperlin, G. Ligresti, M.B. Hilscher, et al., Mechanosensing and fibrosis, *J. Clin. Invest.* 128 (2018) 74–84.
- [12] T.A. Wynn, Fibrotic disease and the T(H)1/T(H)2 paradigm, *Nat. Rev. Immunol.* 4 (2004) 583–594.
- [13] P. Zerr, K. Palumbo-Zerr, J. Huang, et al., Sirt1 regulates canonical TGF-beta signalling to control fibroblast activation and tissue fibrosis, *Ann. Rheum. Dis.* 75 (2016) 226–233.
- [14] R.A. Cahill, Prevention of intra-abdominal adhesions using the antiangiogenic COX-2 inhibitor celecoxib, *Ann. Surg.* 244 (2006) 327–328, author reply 328.
- [15] H. Bora, S.V. Aykol, N. Akyurek, et al., Inhibition of epidural scar tissue formation after spinal surgery: external irradiation vs. spinal membrane application, *Int. J. Radiat. Oncol. Biol. Phys.* 51 (2001) 507–513.
- [16] F. Zhang, K. Liu, Z. Pan, et al., Effects of rosiglitazone/PHEBV drug delivery system on postoperative fibrosis in rabbit glaucoma filtration surgery model, *Drug Deliv.* 26 (2019) 812–819.
- [17] M.L. Hautekeete, G. Babany, P. Marcellin, et al., Retroperitoneal fibrosis after surgery for aortic aneurysm in a patient with periarteritis nodosa: successful treatment with corticosteroids, *J. Intern. Med.* 228 (1990) 533–536.
- [18] J.I. Jun, L.F. Lau, Resolution of organ fibrosis, *J. Clin. Invest.* 128 (2018) 97–107.
- [19] N.K. Karamanos, A.D. Theocharis, T. Neill, et al., Matrix modeling and remodeling: a biological interplay regulating tissue homeostasis and diseases, *Matrix Biol.* 75–76 (2019) 1–11.
- [20] J. Massague, TGFbeta signalling in context, *Nat. Rev. Mol. Cell Biol.* 13 (2012) 616–630.
- [21] A. Leask, D.J. Abraham, TGF-beta signaling and the fibrotic response, *Faseb. J.* 18 (2004) 816–827.
- [22] R. Strippoli, J. Loureiro, V. Moreno, et al., Caveolin-1 deficiency induces a MEK-ERK1/2-Snail-1-dependent epithelial-mesenchymal transition and fibrosis during peritoneal dialysis, *EMBO Mol. Med.* 7 (2015) 102–123.
- [23] F. Liu, D. Lagares, K.M. Choi, et al., Mechanosignaling through YAP and TAZ drives fibroblast activation and fibrosis, *Am. J. Physiol.-Lung C.* 308 (2015) L344–L357.
- [24] N.I. Chaudhary, G.J. Roth, F. Hilberg, et al., Inhibition of PDGF, VEGF and FGF signalling attenuates fibrosis, *Eur. Respir. J.* 29 (2007) 976–985.
- [25] H. Xie, D. Xie, J. Zhang, et al., ROS/NF-kappaB signaling pathway-mediated transcriptional activation of TRIM37 promotes HBV-associated hepatic fibrosis, *Mol. Ther. Nucleic Acids* 22 (2020) 114–123.
- [26] R.A. Moore, S. Derry, D. Aldington, et al., Single Dose Oral Analgesics for Acute Postoperative Pain in Adults - an Overview of Cochrane Reviews, *Cochrane Database Syst Rev*, 2015. CD008659.
- [27] M. Regulska, K. Regulska, W. Prukala, et al., COX-2 inhibitors: a novel strategy in the management of breast cancer, *Drug Discov. Today Off.* 21 (2016) 598–615.
- [28] K. Richter, A. Konzack, T. Pihlajaniemi, et al., Redox-fibrosis: impact of TGFbeta1 on ROS generators, mediators and functional consequences, *Redox Biol* 6 (2015) 344–352.
- [29] J.A. Mitchell, N.S. Kirkby, B. Ahmetaj-Shala, et al., Cyclooxygenases and the cardiovascular system, *Pharmacol. Ther.* (2020), 107624.
- [30] R. Niranjani, K.P. Mishra, A.K. Thakur, Inhibition of cyclooxygenase-2 (COX-2) initiates autophagy and potentiates MPTP-induced autophagic cell death of human neuroblastoma cells, SH-SY5Y: an inside in the pathology of Parkinson's disease, *Mol. Neurobiol.* 55 (2018) 8038–8050.
- [31] T. Bryn, S. Yaqub, M. Mahic, et al., LPS-activated monocytes suppress T-cell immune responses and induce FOXP3+ T cells through a COX-2-PGE2-dependent mechanism, *Int. Immunol.* 20 (2008) 235–245.
- [32] M. Tsujii, R.N. DuBois, Alterations in cellular adhesion and apoptosis in epithelial cells overexpressing prostaglandin endoperoxide synthase 2, *Cell* 83 (1995) 493–501.
- [33] R. Chou, D.B. Gordon, O.A. de Leon-Casasola, et al., Management of postoperative pain: a clinical practice guideline from the American pain society, the American society of regional anesthesia and pain medicine, and the American society of anesthesiologists' committee on regional anesthesia, executive committee, and administrative council, *J. Pain* 17 (2016) 131–157.
- [34] G. Varrassi, C.T. Yeam, M. Rekasina, et al., The Expanding Role of the COX Inhibitor/Opioid Receptor Agonist Combination in the Management of Pain, *Drugs*, 2020.
- [35] A. Buvanendran, J.S. Kroin, K.J. Tuman, et al., Effects of perioperative administration of a selective cyclooxygenase 2 inhibitor on pain management and recovery of function after knee replacement: a randomized controlled trial, *J. Am. Med. Assoc.* 290 (2003) 2411–2418.
- [36] J.D. Kelly, W.S. Tan, N. Porta, et al., BOXIT-A randomised phase III placebo-controlled trial evaluating the addition of celecoxib to standard treatment of transitional cell carcinoma of the bladder (CRUK/07/004), *Eur. Urol.* 75 (2019) 593–601.
- [37] S. Giacchetti, A.S. Hamy, S. Delalogue, et al., Long-term outcome of the REMAGUS 02 trial, a multicenter randomised phase II trial in locally advanced breast cancer patients treated with neoadjuvant chemotherapy with or without celecoxib or trastuzumab according to HER2 status, *Eur. J. Canc.* 75 (2017) 323–332.
- [38] P.A. Thompson, E.L. Ashbeck, D.J. Roe, et al., Celecoxib for the prevention of colorectal adenomas: results of a suspended randomized controlled trial, *J. Natl. Cancer Inst.* 108 (2016).
- [39] P.M. Lynch, C.A. Burke, R. Phillips, et al., An international randomised trial of celecoxib versus celecoxib plus difluoromethylornithine in patients with familial adenomatous polyposis, *Gut* 65 (2016) 286–295.
- [40] M.I. Husain, I.B. Chaudhry, A.B. Khoso, et al., Minocycline and celecoxib as adjunctive treatments for bipolar depression: a multicentre, factorial design randomised controlled trial, *Lancet Psychiatr.* 7 (2020) 515–527.
- [41] N.D. Yeomans, D.Y. Graham, M.E. Husni, et al., Randomised clinical trial: gastrointestinal events in arthritis patients treated with celecoxib, ibuprofen or naproxen in the PRECISION trial, *Aliment. Pharmacol. Ther.* 47 (2018) 1453–1463.
- [42] J.H. Gao, S.L. Wen, S. Feng, et al., Celecoxib and octreotide synergistically ameliorate portal hypertension via inhibition of angiogenesis in cirrhotic rats, *Angiogenesis* 19 (2016) 501–511.
- [43] L. Li, X. Zheng, D. Fan, et al., Release of celecoxib from a bi-layer biomimetic tendon sheath to prevent tissue adhesion, *Mater Sci Eng C Mater Biol Appl* 61 (2016) 220–226.
- [44] S. Jiang, X. Zhao, S. Chen, et al., Down-regulating ERK1/2 and SMAD2/3 phosphorylation by physical barrier of celecoxib-loaded electrospun fibrous membranes prevents tendon adhesions, *Biomaterials* 35 (2014) 9920–9929.
- [45] A.K. Greene, I.P. Alwayn, V. Nose, et al., Prevention of intra-abdominal adhesions using the antiangiogenic COX-2 inhibitor celecoxib, *Ann. Surg.* 242 (2005) 140–146.
- [46] Y.H. Paik, J.K. Kim, J.I. Lee, et al., Celecoxib induces hepatic stellate cell apoptosis through inhibition of Akt activation and suppresses hepatic fibrosis in rats, *Gut* 58 (2009) 1517–1527.
- [47] P.A. Gagliardi, A. Puliafito, L. Primo, PDK1: at the crossroad of cancer signaling pathways, *Semin. Canc. Biol.* 48 (2018) 27–35.
- [48] C.H. Chan, U. Jo, A. Kohrman, et al., Posttranslational regulation of Akt in human cancer, *Cell Biosci.* 4 (2014) 59.
- [49] W. Li, C. Peng, M.H. Lee, et al., TRAF4 is a critical molecule for Akt activation in lung cancer, *Canc. Res.* 73 (2013) 6938–6950.
- [50] M.G. Jones, A. Fabre, P. Schneider, et al., Three-dimensional characterization of fibroblast foci in idiopathic pulmonary fibrosis, *JCI Insight* 1 (2016).
- [51] H. Xia, A. Gilbertsen, J. Herrera, et al., Calcium-binding protein S100A4 confers mesenchymal progenitor cell fibrogenicity in idiopathic pulmonary fibrosis, *J. Clin. Invest.* 127 (2017) 2586–2597.
- [52] S.P. Giblin, A. Schwenzer, K.S. Midwood, Alternative splicing controls cell lineage-specific responses to endogenous innate immune triggers within the extracellular matrix, *Matrix Biol.* 00 (2020) 1–20.
- [53] J. Prakash, M. Pinzani, Fibroblasts and extracellular matrix: targeting and therapeutic tools in fibrosis and cancer, *Adv. Drug Deliv. Rev.* 121 (2017) 1–2.
- [54] M.C. Lampi, C.A. Reinhart-King, Targeting extracellular matrix stiffness to attenuate disease: from molecular mechanisms to clinical trials, *Sci. Transl. Med.* 10 (2018).
- [55] J. Massague, J. Seoane, D. Wotton, Smad transcription factors, *Genes Dev.* 19 (2005) 2783–2810.
- [56] G. Vietti, S. Ibouaadata, M. Palmal-Pallag, et al., Towards predicting the lung fibrogenic activity of MWCNT: key role of endocytosis, kinase receptors and ERK 1/2 signaling, *Nanotoxicology* 10 (2016) 488–500.
- [57] A.J. Haak, E. Kostallari, D. Sicard, et al., Selective YAP/TAZ inhibition in fibroblasts via dopamine receptor D1 agonism reverses fibrosis, *Sci. Transl. Med.* 11 (2019).
- [58] T.A. Wynn, K.M. Vannella, Macrophages in tissue repair, regeneration, and fibrosis, *Immunity* 44 (2016) 450–462.
- [59] M.L. Bochaton-Piallat, G. Gabbiani, B. Hinz, The Myofibroblast in Wound Healing and Fibrosis: Answered and Unanswered Questions, 2016. F1000Res 5.
- [60] S. Jia, M. Agarwal, J. Yang, et al., Discoidin domain receptor 2 signaling regulates fibroblast apoptosis through PDK1/akt, *Am. J. Respir. Cell Mol. Biol.* 59 (2018) 295–305.
- [61] D.J. Wilkinson, M. Piasecki, P.J. Atherton, The age-related loss of skeletal muscle mass and function: measurement and physiology of muscle fibre atrophy and muscle fibre loss in humans, *Ageing Res. Rev.* 47 (2018) 123–132.
- [62] R.Y. Cao, J. Li, Q. Dai, et al., Muscle atrophy: present and future, *Adv. Exp. Med. Biol.* 1088 (2018) 605–624.
- [63] A. Gupta, M. Bah, NSAIDs in the treatment of postoperative pain, *Curr. Pain Headache Rep.* 20 (2016) 62.
- [64] P. Fabbri, M.N. Schilte, M. Zareie, et al., Celecoxib treatment reduces peritoneal fibrosis and angiogenesis and prevents ultrafiltration failure in experimental peritoneal dialysis, *Nephrol. Dial. Transplant.* 24 (2009) 3669–3676.
- [65] P.X. Zhang, J. Cheng, S. Zou, et al., Pharmacological modulation of the AKT/microRNA-199a-5p/CAVI1 pathway ameliorates cystic fibrosis lung hyperinflammation, *Nat. Commun.* 6 (2015) 6221.
- [66] A.Y. Hui, A.J. Dannenberg, J.J. Sung, et al., Prostaglandin E2 inhibits transforming growth factor beta 1-mediated induction of collagen alpha 1(I) in hepatic stellate cells, *J. Hepatol.* 41 (2004) 251–258.
- [67] A.S. Hamy, S. Tury, X. Wang, et al., Celecoxib with neoadjuvant chemotherapy for breast cancer might worsen outcomes differentially by COX-2 expression and ER status: exploratory analysis of the REMAGUS02 trial, *J. Clin. Oncol.* 37 (2019) 624–635.
- [68] M.J. Edelman, L. Hodgson, X. Wang, et al., Cyclooxygenase-2 (COX-2) as a predictive marker for the use of COX-2 inhibitors in advanced non-small-cell lung cancer, *J. Clin. Oncol.* 30 (2012) 2019–2020. ; author reply 2020.
- [69] J. Tian, F. Guo, Y. Chen, et al., Nanoliposomal formulation encapsulating celecoxib and genistein inhibiting COX-2 pathway and Glut-1 receptors to prevent prostate cancer cell proliferation, *Canc. Lett.* 448 (2019) 1–10.

- [70] P. Li, H. Wu, H. Zhang, et al., Aspirin use after diagnosis but not prediagnosis improves established colorectal cancer survival: a meta-analysis, *Gut* 64 (2015) 1419–1425.
- [71] M. Zhang, D. Fraser, A. Phillips, Erk, p38, and Smad signaling pathways differentially regulate transforming growth factor-beta1 autoinduction in proximal tubular epithelial cells, *Am. J. Pathol.* 169 (2006) 1282–1293.
- [72] A. Dey, X. Varelas, K.L. Guan, Targeting the Hippo pathway in cancer, fibrosis, wound healing and regenerative medicine, *Nat. Rev. Drug Discov.* 19 (2020) 480–494.
- [73] J.H. Chen, C.J. Perry, Y.C. Tsui, et al., Prostaglandin E2 and programmed cell death 1 signaling coordinately impair CTL function and survival during chronic viral infection, *Nat. Med.* 21 (2015) 327–334.
- [74] X. Sun, Z. Xie, B. Hu, et al., The Nrf2 activator RTA-408 attenuates osteoclastogenesis by inhibiting STING dependent NF-kappaB signaling, *Redox Biol* 28 (2020), 101309.
- [75] S.V. Silva, M.A. Lima, N. Cella, et al., ADAMTS-1 is found in the nuclei of normal and tumoral breast cells, *PLoS One* 11 (2016) e0165061.
- [76] L. Casares, V. Garcia, M. Garrido-Rodriguez, et al., Cannabidiol induces antioxidant pathways in keratinocytes by targeting BACH1, *Redox Biol* 28 (2020), 101321.